

## STELLAR AND DUST PROPERTIES IN A SAMPLE OF BLUE EARLY TYPE GALAXIES

S. P. Deshmukh<sup>1</sup>, N. D. Vagshette<sup>2</sup> and M. K. Patil<sup>3</sup>

<sup>1</sup>*Department of Physics, Institute of Science, civil lines, Nagpur-440001, India*  
E-mail: [phy.deshmukh@iscnagpur.ac.in](mailto:phy.deshmukh@iscnagpur.ac.in)

<sup>2</sup>*Department of Physics and Electronics, Maharashtra Udaygiri Mahavidyalaya, Udgir, Latur-413517, India*  
E-mail: [nilkanth1384@gmail.com](mailto:nilkanth1384@gmail.com)

<sup>3</sup>*Swami Ramanand Teerth Marathwada University, Nanded 631 606, India*  
E-mail: [patil@associates.iucaa.in](mailto:patil@associates.iucaa.in)

(Received: February 22, 2022; Accepted: September 19, 2022)

**SUMMARY:** This paper presents a comparative study of physical properties of a sample of 89 blue early-type galaxies (ETGs) from the local universe by fitting SEDs to their multi-wavelength photometric and spectroscopic data. The detailed template-based SED fitting analysis using the *MAGPHYS* and *SED3FIT* codes on the interstellar dust extinction corrected UV-to-far-IR spectro-photometric data enabled us to trace the evolutionary sequence of the blue ETGs on the color-magnitude diagram. This study evidenced a decreasing trend of the SFR, sSFR, dust mass, and dust mass fraction over the sequence from the SF - to - the Seyferts - to - the LINERs. The UV-optical colors also enabled us to estimate the look-back time of the last starburst phase in SF, Seyfert, and LINER galaxies, probably pointing towards the evolutionary sequence of the blue ETGs. Despite the blue colors and strong emission lines in the optical regime of the electromagnetic spectrum, the blue ETGs in the present sample occupy a position off the main sequence, commonly known as the *green valley*, on the CMD plot and hence indicate the transitional state of their non-secular evolution. A marginal positive correlation was noticed between SFR per unit dust mass and the temperature of the cool ISM. The declining trend of the cold dust temperature  $T_c$  over the sequence from the SF-to-Seyfert-to-LINER implies that the AGNs in the systems are not enough powerful to affect the cold component of the ISM.

**Key words.** Galaxies: star formation – Galaxies: elliptical and lenticular, cD

### 1. INTRODUCTION

Early type galaxies (ETGs), ellipticals and lenticulars together, were thought to be "red & dead" systems that evolve passively following a tight color-magnitude relation populating along the "red sequence" on the color-magnitude diagram (CMD)

of galaxies (Faber 1973, Visvanathan and Sandage 1977). In the pioneering work on the CMD of early-type galaxies Baum (1959) observed that the colors of these galaxies become bluer as they become less luminous. The evident color-magnitude relation is, in general, attributed to the metallicity effect of the hosts (Kodama and Arimoto 1997). A general scenario is that a galaxy moves on the CMD plane from the "blue-cloud" region, a region occupied by the actively star-forming, young, morphologically late type galaxies, to the non-starforming, passive red ETGs.

---

© 2022 The Author(s). Published by Astronomical Observatory of Belgrade and Faculty of Mathematics, University of Belgrade. This open access article is distributed under CC BY-NC-ND 4.0 International licence.

The quenching of the star-formation in ETGs is likely either due to the removal or heating of the cold gas supply essential for the star formation. However, this is not the sole fate of the ETGs. Based on various multi-wavelength surveys and missions involved in recent studies, it has been realized that a countable fraction of ETGs exhibit offset to this red sequence on the CMD plane and possess relatively bluer colors (Faber *et al.* 2007, Kannappan *et al.* 2009, Yi *et al.* 2005).

The blue ETGs not only differ in color from their red-sequence cousins of ETGs but there are several other factors that confirm their distinction. One of the key parameters is related to their distribution in space in the sense that the blue ETGs normally are seen more abundantly in the low-density environment with lower values of velocity dispersions (Schawinski *et al.* 2009). Additionally, such systems were found to possess nonsymmetric color distribution (Lee *et al.* 2006) with a positive color gradient i.e. bluer centers unlike the common red ETGs (Ge and Gu 2012). This is in contrast to the text-book view of the ETGs, where they were characterized to be comprised of old populations stars and a total devoid of gas and dust. However, deep imaging observations of a large sample of galaxies over the past five decades have demonstrated that a significant fraction of ETGs host multi-phase ISM like, neutral, molecular gas, dust (Knapp *et al.* 1989, Ebner and Balick 1985, Goudfrooij *et al.* 1994a, Patil *et al.* 2007, Vagshette *et al.* 2012, Deshmukh *et al.* 2013) and ionized gas (Osterbrock 1960, Goudfrooij *et al.* 1994b). The origin of this component of ISM was believed to be due to the mass-loss from the old stars, which may be utilized by the galaxies for star formation. However, the quantum of the ISM in general and interstellar dust in particular evidenced in these galaxies via optical extinction measurements was higher by several orders of magnitude compared to that estimated through the dust mass build-up of the host assuming observed mass loss rates (Dewangan *et al.* 1999, Patil *et al.* 2007). Further, the extent and morphologies of the dust evident in the dusty ETGs provided the direct evidences in support of a major fraction of it must have been acquired by the host externally either through a merger or tidal-capture. The process that brings back the red & dead systems back to the blue cloud are either the star formation or the active phase of the AGN (Lee *et al.* 2006, Kannappan *et al.* 2009, Rowlands *et al.* 2012). However, the role of the central AGN on accelerating star formation in the host galaxy does not have convincing evidences. A consensus is that the AGN suppresses the star formation in the host either by expelling or heating the ingredient required for star formation (Fabian 2012). An increasing population of the AGN hosting galaxies in the green-valley, the transition region separating the blue cloud from the red sequence, strengthens our belief that the star formation is being quenched through the negative feedback of the AGN.

On the other side, a correlation has been witnessed between the rates of black hole accretion (BHAR) and the star formation (SFR) in some star-forming galaxies (Chen and Hickox 2014) and Seyfert galaxies (Diamond-Stanic and Rieke 2012). Similarly, some of the star-burst galaxies revealed a high rate of BHAR relative to the main-sequence galaxies, while systems with no BHAR appeared as the quiescent galaxies (Rodighiero *et al.* 2015). Luminous X-ray detected AGNs were also noticed to show higher SFRs (Rafferty *et al.* 2011). Nonetheless, the mode how star formation is triggered in the blue ETGs residing in loose fields is under debate.

The necessary ingredient for the star formation that turns them into blue ETGs is found to be acquired externally through a minor merger like episode (Schweizer and Seitzer 1992, Serra and Oosterloo 2010, Kaviraj *et al.* 2011). Minor mergers in low-density regions can inject a sufficient amount of gas and hence induce star formation in an otherwise gas-poor ETG. Confirmation of this was provided by the radio surveys of relaxed nearby ETGs, which have revealed a significant fraction of cold molecular gas ( $\sim 10^7 - 10^9 M_{\odot}$ ) in the blue ETGs (Wei *et al.* 2010, Young *et al.* 2011, Stark *et al.* 2013, Davis *et al.* 2019). This component of the cold ISM was attributed to originate from the external sources like minor merger of gas-rich galaxies and plays a significant role in the evolution of the galaxies (Morganti *et al.* 2006, Oosterloo *et al.* 2010). The externally acquired cold gas initiates the star-formation in the galaxy in action and makes it to migrate from the red sequence back to the blue cloud on the color-magnitude diagram of galaxies. The evidences in support of this were provided by several researchers (e.g. Kannappan *et al.* 2009, Huertas-Company *et al.* 2010, Marino *et al.* 2011, McIntosh *et al.* 2014, Rutkowski *et al.* 2014, Wong *et al.* 2015). Though the origin of fuel for the star formation in these galaxies is not fully understood, there are several evidences in support of its external origin through a merger like or flyby episode (Patil *et al.* 2007). The signatures of such merger events are confirmed through the imaging and structural analysis in numerous systems (Goudfrooij *et al.* 1994b, Patil *et al.* 2007, Finkelman *et al.* 2012). As a result, there is a need to investigate the star formation in this class of galaxies, which otherwise were believed to be passively evolving *red-and-dead* systems.

Schawinski *et al.* (2007) while working on the morphologically identified early type galaxies as a part of the MOSES project noticed a systematic pattern on the color-velocity dispersion diagram pointing towards a possible evolutionary sequence of the ETGs as the star-forming (SF) galaxies to the AGN-SF composites, the Seyferts, the LINER terminating into the quiescent galaxies. Inspired with this study, the present paper is aimed to investigate the trend of the star formation as a function of their activity class in a sample of blue ETGs. This paper also attempts to

carry out the quantitative and comparative study of dust content, dust properties and stellar content of the targets as a function of the activity class. As the spectral energy distribution (SED) of galaxies acts as the most direct probe for galaxy properties, therefore, we use the template-based fitting approach to the multi-wavelength photometric and spectroscopic data on targets acquired using various missions like the Sloan Digital Sky-Survey Data Release 6 (SDSS DR6), the GALEX, the Two Micron All Sky Survey (2MASS), the Wide-field Infrared Survey (WISE), the Infrared Astronomical Satellite (IRAS), etc.

This paper is organized as follows: Section 2 presents the sample selection, data acquisition and analysis. Section 3 presents the main results and discussion on them, while Section 4 summarises our findings. Throughout the work, we adopt a flat cosmological model with  $\Omega_M = 0.3$ ,  $\Omega_\Lambda = 0.7$  and  $H_0 = 70$  km s<sup>-1</sup> and use the initial mass function of Chabrier (2003).

## 2. SAMPLE SELECTION AND DATA ANALYSIS

### 2.1. Sample selection

The galaxy sample for the present study is the subset of 204 blue ETGs of Schawinski et al. (2009) (hereafter S2009). The S2009 galaxies were derived from the public photometric and spectroscopic data products available in the Sloan Digital Sky Survey (SDSS) Data Release 6 (York et al. 2000) that include galaxies with spectroscopic redshift range over  $0.02 < z < 0.05$  and is limited to the absolute r-band PetroMag magnitude  $M_{r,\text{Petro}} < -20.7$ . The details of the sample selection and underlying properties are described in Schawinski et al. (2009). To cover morphologically different classes of ETGs this volume-limited sample was further shortlisted by employing the Galaxy Zoo Clean catalog (Lintott et al. 2008). This enabled them to select a set of 3588 ETGs, out of which S2009 considered extreme blue ETGs by plotting the  $(u-r)$  optical color vs magnitude graph and fitting Gaussian to the  $(u-r)$  color with a magnitude bin of  $dM=0.33$  mag. Here, the blue ETGs were identified as the galaxies that reside below  $3\sigma$  offset to the red sequence. Following to which they derive a sample of 204 blue ETGs that make up  $5.7 \pm 0.4\%$  of the total volume limited local population. S2009 noticed comparatively low velocity dispersions for these blue ETGs and were found to reside in the low-density environments. Based on the SDSS optical spectrum and making use of the BPT diagram S2009 noticed that out of 204 blue ETGs, 24.5% are of the star-forming class, 25.5% composites, 7.4% Seyferts and about 5.4% of the LINERs. The remaining 37.3% of galaxies exhibited weak emission lines as a result these were not included in S2009. Out of these 204, we have considered only star-forming (SFs) and AGNs, thus making a sample of 89 blue ETGs for the

present study. Out of 89, 55 are SFs, 20 are Seyferts and remaining 14 are the LINERs.

### 2.2. Data acquisition

For the present study, we have used optical photometric as well as spectroscopic data from the SDSS DR6 in the  $u, g, r, i$  and  $z$  passbands for the sample of 89 blue ETGs considering their Petrosian magnitudes (Abazajian et al. 2009). As Ultraviolet (UV) light in a galaxy predominantly originates from the newly formed massive stars, the UV observations of these galaxies act as an excellent probe for the current star formation. Therefore, for a better understanding of the star formation in the sample galaxies, we have made use of the Near-UV and Far-UV passband data from the *Galaxy Evolution Explorer* (GALEX) space mission. These measurements were calibrated to the AB magnitude system of Oke and Gunn (1983) using the GALEX pipeline. To cover the near-infrared data in the J, H and Ks (Kron magnitudes) passbands of the electromagnetic spectrum, we use Two Micron All Sky Survey (2MASS) Extended Source Catalog (EXC) (Skrutskie et al. 2006) and for the mid-IR data we use the Wide-field Infrared Survey (WISE) (Wright et al. 2010) W1, W2, W3 and W4 passbands considering their  $wgmag$  magnitudes. We used the *Infrared Astronomical Satellite* (IRAS; Beichman et al. 1988) faint source catalog data for far-IR observations. The SDSS, 2MASS, and WISE magnitudes were converted to the AB magnitudes and were corrected for the Galactic dust extinction using the Schlegel et al. (1998) reddening maps at  $R_V = 3.1$  Cardelli et al. (1989) extinction law.

As the sample for the present study includes star-forming as well as AGNs, therefore, the nebular emission lines centered at the  $H_\alpha$ ,  $H_\beta$ , forbidden Oxygen and Nitrogen lines in the optical region may have considerable contribution in the SDSS  $u, g, r$  magnitudes. To obtain the true continuum flux free from the nebular emission contribution, we used the *REMOVEYOUNG* spectral synthesis code of Gomes and Papaderos (2016). This code utilizes stellar population vector information generated by the *STARLIGHT* V 04 SPS model as an input (Cid Fernandes et al. 2005, Mateus et al. 2007). For spectral fitting of the Seyfert and LINER galaxies from our sample we use a linear combination of 45 SSP models from Bruzual and Charlot (2003) corresponding to the metallicity values of  $Z = 0.2, 1, 2.5 Z_\odot$  that comprises 15 different stellar age combinations as 0.001, 0.00316, 0.005, 0.01, 0.025, 0.04, 0.102, 0.286, 0.640, 0.905, 1.434, 2.5, 5, 11, and 13 Gyr. We also used an extra power law with the coefficient  $\beta = -1.5$  (Cid Fernandes et al. 2004) for fitting spectra of these galaxies. The multi-wavelength continuum flux free from the nebular emission contribution was then used for further analysis. We used the code *STARLIGHT* to obtain the underlying stellar absorption free  $H_\alpha$  and  $H_\beta$  emission line flux densities and used them for quantifying star formation rates.

### 2.3. Modelling galaxy SEDs

The energy output of a galaxy spans over the entire electromagnetic spectrum. Barring the galaxies whose emission is dominated by mass accretion onto the supermassive black holes at their center, the UV to IR emission from nearly all the galaxies in the universe is originating from the constituent stars. This radiation during its propagation through the galaxy is likely reprocessed by the dust and gas (ISM together) and, hence, inevitably carries imprints of these processes. Thus, the UV-to-IR spectral energy distribution of a galaxy provides a wealth of information about the constituent stars and the total ISM content of the galaxy. Therefore, the use of the multi-wavelength data on a galaxy enables us to construct a distribution of the collected energy as a function of wavelength, commonly referred to as the spectral energy distribution (SED). Such a distribution can be compared with those of the well-studied objects by deriving their template-based models. Matching of the two SEDs enables us to assume that the observed object resembles the identical physical characteristics as that of the object. Here, the SEDs of the well-known objects are the templates and can be used as standards for constraining the properties of the objects under study. As a result, we have made attempts to derive SEDs of the target galaxies employing multi-wavelength datasets on each of them acquired from different observatories. The modeling of the observed SEDs of target galaxies was done using the publicly available "Multi-wavelength Analysis of Galaxy Physical Properties" (MAGPHYS) (da Cunha *et al.* 2008) code, which interprets the broadband spectral energy distribution of sample galaxies and enables us to derive various physical parameters of the program galaxies. MAGPHYS utilizes several libraries to develop a template that matches with the observed SED and hence delivers various parameters like its stellar mass, star formation rate, specific star formation rate, dust luminosity, etc. To constrain the optical portion of the electromagnetic spectrum the library developed by Bruzual and Charlot (2003) considers about 50,000 different models of varying stellar populations in optical region and the IR library comprises 50,000 models that represent an optically thin modified black body emission due to its interaction with dust grains of different sizes, temperature, and emissivity indices.

We prefer the two-component dust model developed by Charlot and Fall (2000) to cover the attenuation effect of the starlight by interstellar dust. For a given redshift of the program galaxy, MAGPHYS builds a discrete set of randomly selected model libraries assuming stochastic star-related and dust-related properties. This model SED was then compared with the observed SED to test how well it constrains the observed galaxy properties. The final well-fit model was derived by employing the  $\chi^2$  minimization and examining the goodness of fit. As the accretion of matter onto the supermassive black hole at

the center of the galaxy can additionally contribute to the observed UV/Optical/IR SED of it, therefore, we used the SED3FIT code of Berta *et al.* (2013) for the fitting purpose. This code considers all the three emission components (i.e., stars, dust and AGN) of a galaxy by combining MAGPHYS model with the Torus library introduced by Fritz *et al.* (2006). The Torus library includes 10 different models that cover the entire range of the spectrum. Among the two fitted SEDs, we selected the best-fitted model that satisfies the Fisher test (Bevington and Robinson 2003) expressed as:

$$F_{\text{test}} = \frac{\chi_{\text{noagn}}^2 - \chi_{\text{agn}}^2}{\chi_{\nu,\text{agn}}^2} \geq F_{\text{threshold}}(CL), \quad (1)$$

where  $\chi_{\text{noagn}}^2$  and  $\chi_{\text{agn}}^2$  are the  $\chi^2$  values of the best fit SEDs with AGN (SED3FIT) and without AGN (MAGPHYS), respectively,  $\chi_{\nu,\text{agn}}^2$  represent the reduced  $\chi^2$  value corresponding to the best fit with AGN contribution.  $F_{\text{threshold}}(CL)$  is the threshold value of the  $\chi^2$  considered for the confidence level of 0.05 and given degrees-of-freedom (*dof*). We calculated the *dof* for each of the system following the procedure outlined in Smith *et al.* (2012). This exercise yielded the best fit with the SED3FIT for 4 star-forming galaxies, 4 Seyfert galaxies and for 1 LINER galaxies. As a result, we used the results from the SED3FIT analysis for these systems for further study. Thus, the robustness of the MAGPHYS and SED3FIT codes depends on the  $\chi^2$  values and, hence, on the selected optical/IR/Torus models. We finally verify the robustness of the fitted SEDs for our sample galaxies using the *p*-value that depends on the measured  $\chi^2$  values and the *dof* (Clauset *et al.* 2009). Here, the *p*-value quantifies the possibility of the null hypothesis and represents the significance of the fit. The histogram of the resultant *p*-value of the best fitted SEDs at a significance level 0.05 is shown in Fig. 1 and reveals a peak near 100 (in percentage) confirming that the quality of the SED fit is appreciable.

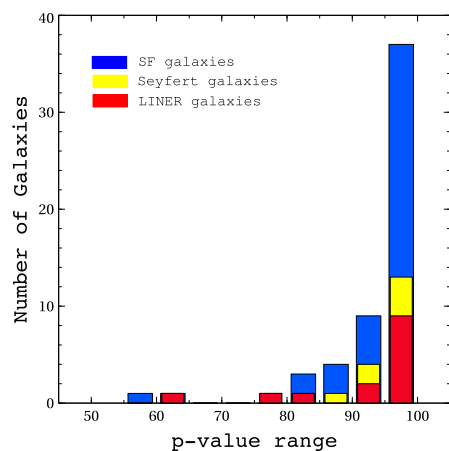


Fig. 1: Histogram of *p*-values for the sample galaxies.

### 3. RESULTS AND DISCUSSION

#### 3.1. Star formation rates

Star formation rate (SFR) is the key component to investigate the evolution of galaxies and can be estimated using various methods. The UV-Optical-IR SED fitting for the sample galaxies performed employing the MAGPHYS and the SED3FIT codes. The average SFR thus estimated for the star-forming galaxies from our sample ranges over  $(0.03 - 9.13) M_{\odot} \text{ yr}^{-1}$  is with an average of  $0.83 M_{\odot} \text{ yr}^{-1}$ , while the average values of SFR for the Seyfert and LINER galaxies were found to be  $0.70 M_{\odot} \text{ yr}^{-1}$  and  $0.29 M_{\odot} \text{ yr}^{-1}$ , respectively.

We also estimate the SFR in target galaxies using the SDSS DR6 spectra for the sample galaxies. Here, we derive the  $H_{\alpha}$  flux densities for all the SF galaxies by fitting emission lines using the STARLIGHT code. Before this, the spectra were shifted to the rest frames and were also corrected for the Galactic extinction. The STARLIGHT fitted residual spectra were employed to measure the emission line flux densities using the *deblending* task of IRAF. Each of the observed emission lines was fitted with the Gaussian profile and the SFRs were estimated using the [Kennicutt \(1998\)](#)'s relation scaled to [Chabrier \(2003\)](#),

$$SFR = \frac{L(H_{\alpha})}{2.1 \times 10^{41}} M_{\odot}/\text{yr}, \quad (2)$$

here,  $L(H_{\alpha})$  represents the  $H_{\alpha}$  emission line luminosity quantified as:

$$L(H_{\alpha}) = 4\pi D_l^2 F_{H_{\alpha}} 10^{-0.4(r_{\text{Petro}} - r_{\text{fiber}})} \text{ ergs/sec}, \quad (3)$$

where,  $D_l$  is the galaxy luminosity distance,  $F_{H_{\alpha}}$  the  $H_{\alpha}$  emission line flux. Here the  $H_{\alpha}$  emission line flux was corrected for the interstellar dust and stellar absorption following [Hopkins et al. \(2003\)](#). The aperture correction for the observed flux values was achieved using the factor  $10^{-0.4(r_{\text{Petro}} - r_{\text{fiber}})}$ . The SFRs for the SF galaxies estimated using both methods i.e., from the spectroscopic flux densities and the SED fitting, are compared and the correlation between them is shown in Fig. 2. This figure confirms an agreement between the two estimates. We excluded the Seyfert and LINER systems from this correlation due to the reason that the flux densities are strongly contaminated by the emission from the central AGN.

#### 3.2. Main sequence relationship

Star-forming galaxies that follow the secular evolution exhibit a very tight relationship between the SFR and the stellar mass  $M_{\text{star}}$  content of the galaxy and is regarded as the main sequence (MS). On the other hand, the galaxies that experience the stochastic mode of star formation are the outliers of the MS relation in the sense that the galaxies with intense star formation lie above the MS, while quiescent

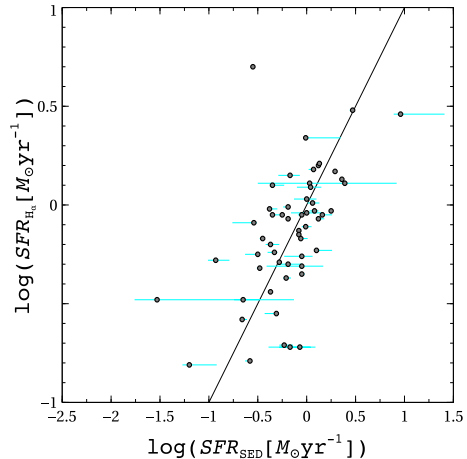


**Fig. 2:** Correlation between the SFRs estimated using the SED fitting versus those estimated from the  $H_{\alpha}$  nebular line flux densities for the SF galaxies from our sample. Here the solid line represents 1:1 relation.

galaxies lie below the MS. To examine the positions of the galaxies from our sample, we have plotted them on the  $M_{\text{star}} - \text{SFR}$  plane and the resultant plot is shown in Fig. 3 (upper panel). A careful inspection of this plot reveals that the majority of galaxies from our sample, whether they are SF, Seyfert or LINERs, lie off the main-sequence.

Another manifestation of the MS relationship is the correlation between the stellar mass  $M_{\text{star}}$  versus the specific star formation rate (sSFR). The galaxies with  $\log(\text{sSFR}) > -10.8$  exhibit active star formation, while those with  $\log(\text{sSFR}) < -11.8$  belong to the quiescent class ([Salim 2014](#)). The galaxies with the sSFR in the range between  $-11.8$  to  $-10.8$  are referred to as the *green valley* galaxies and are believed to represent the transition zone ([Wyder et al. 2007](#), [Schiminovich et al. 2007](#)) indicative of a two-way flow of the galaxy evolution. Thus, the star formation evident in the green valley objects is either due to a triggered mechanism that allows it to move from the red-sequence to the blue-cloud or may quench star formation due to some internal or external influence forcing it to move downward from the blue cloud to the red-sequence. We plot the position of our target galaxies on this plane in the lower panels of Fig. 3. A careful look at this figure reveals that about 24% SFs, 45% Seyferts and 85% LINER galaxies from the sample exhibit  $\log(\text{sSFR})$  less than  $-10.8$ .

#### 3.3. Dust properties

Interstellar dust plays an important role in shaping the nature of the SED of a galaxy. Particularly, in the case of the star-forming galaxies, the energy radiated by the newly formed stars in star forming clouds is absorbed by the interstellar dust in and around these clouds and is then re-radiated in the form of IR radiation. Thus, the total IR emission from a galaxy is the sum of emissions from the warm dust in the

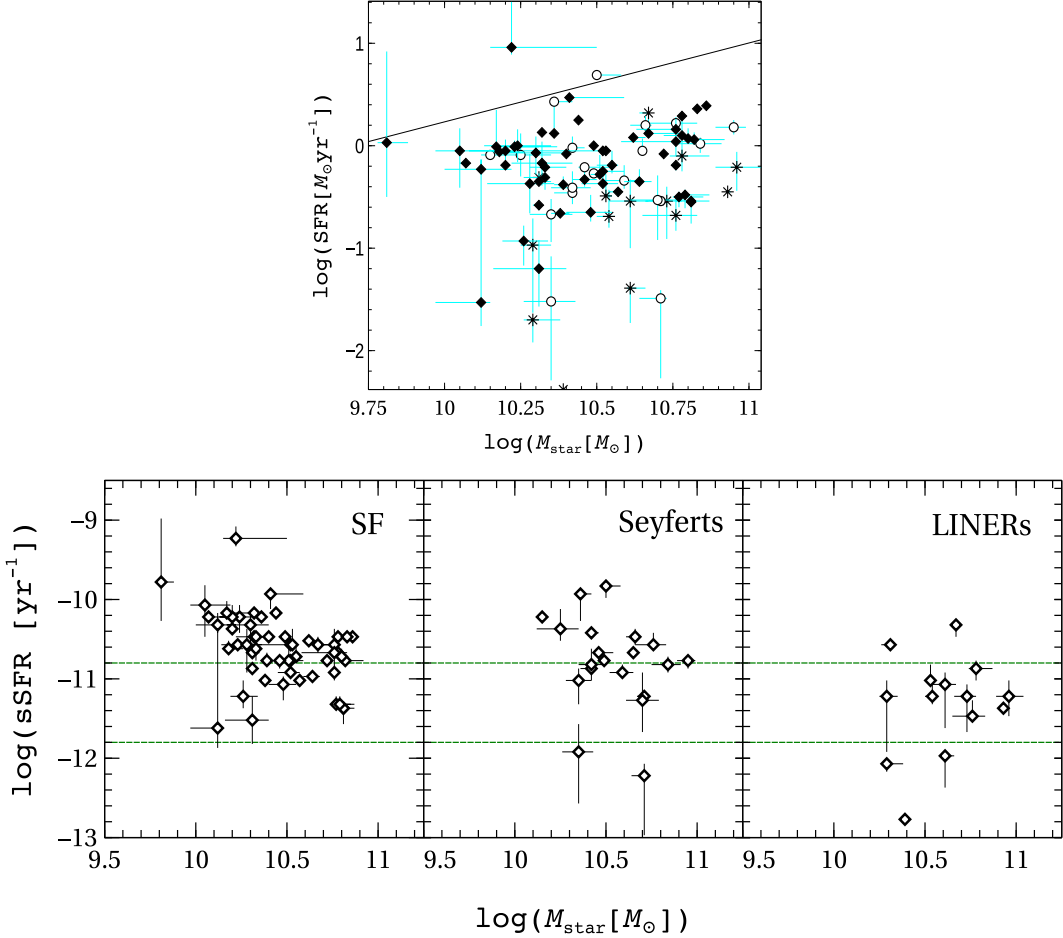


**Fig. 3:** *Upper panel* - The stellar mass content  $M_{\text{star}}$  versus SFR relationship for the program galaxies. The dotted line in this plot represents the Main-sequence of Elbaz *et al.* (2007). All the galaxies from the present sample occupy positions below the main-sequence. Here, the SF galaxies are represented by filled diamonds, Seyferts by open circles and LINERs using the asterisks symbol. *Lower panel* - Distributions of the SF, Seyfert and LINER galaxies in the  $M_{\text{star}}$  versus the specific star formation rate (sSFR) plane. Out of 89 galaxies, 13 SFs, 9 Seyferts and 12 LINERs occupy positions below  $\log(\text{sSFR}) = -10.8$ . The region between dotted lines is known as the *green valley* (Salim 2014).

star-forming clouds and the cool dust that is diffusely distributed throughout the interstellar medium. It is well understood that interstellar dust plays an important role in star formation in host galaxies. As a result, several attempts were made to find a correlation between the star formation and dust content of external galaxies (e.g. Goudfrooij *et al.* 1994, Patil *et al.* 2007). Recent studies by da Cunha *et al.* (2010) of 3258 low-redshift SDSS galaxies have obtained a tight correlation between the SFR and their dust content estimated from the SED fitting. Further confirmation of this was provided by Santini *et al.* (2014), who used the GOODS and COSMOS fields to obtain a strong correlation between the dust content and the SFR for ETGs even at different redshifts. A later study by Hjorth *et al.* (2014) on a much wider sample including that from da Cunha *et al.* (2010) of SDSS as well as Hershel mission revealed that like the

main sequence relation, the  $M_{\text{dust}}$ -SFR relation provides a potential way to investigate the evolutionary sequence of the ETGs. Thus, the total dust content of external galaxies acts as a proxy for the SFR estimation.

The present study of the SED fitting yielded the dust content of the SF, Seyfert and LINER galaxies to be equal to  $1.40 \times 10^7 M_{\odot}$ ,  $1.36 \times 10^7 M_{\odot}$  and  $1.05 \times 10^7 M_{\odot}$ , respectively, about two to three orders of magnitude higher than those estimated for ETGs using optical extinction measurements (Patil *et al.* 2007, Skibba *et al.* 2011, Finkelman *et al.* 2012). However, the estimates of the dust content of this class of galaxies are consistent with those estimated by employing near and far IR data (Patil *et al.* 2007). Further, the results obtained here are consistent with the dust content estimates of blue ETGs detected by the H-ATLAS (Rowlands *et al.* 2012). We have at-

tempted to find a correlation between the star formation rates versus total IR luminosity of the SF galaxies from our sample which is shown in the left panel of Fig. 4. This plot reveals an excess IR luminosity of interstellar dust and low SFR for these galaxies relative to the best-studied correlation (dashed line) by Kennicutt (1998). The excess IR emission from these galaxies implies that the dust grains in the sample galaxies are heated by the radiation field of the old stellar population. The fraction of the IR luminosity due to the dust grains is estimated to be 60%, 65%, and 78% for the SF, Seyfert and LINER galaxies, respectively, relative to their total IR luminosity. We also estimate the fractional dust mass ( $M_{\text{dust}}/M_{\text{star}}$ ) of the target galaxies. It provides an important information on the fraction of dust per unit stellar mass that survives after various destruction processes within galaxies (Calura et al. 2017). We find the fractional dust content for the SF, Seyfert and LINER galaxies to be  $4.29 \times 10^{-4}$ ,  $3.82 \times 10^{-4}$ , and  $2.28 \times 10^{-4}$ , respectively, and is found to be an order of magnitude lower than that observed by da Cunha et al. (2010).

Temperature of dust grains in a galaxy is another important parameter that describes the fate of star formation in them. The cold dust associated with the HI and molecular clouds is supposed to get heated by the radiation field of the old stars. Recent studies by Kirkpatrick et al. (2014) and Clemens et al. (2013) revealed a positive correlation between the SFR normalized over the total dust content of a galaxy versus the cold dust hosted by it. This suggests that young stars in such galaxies play an important role in heating of the cold dust. Here, the underlying assumption is that some of the energetic photons from the star-forming regions emerge out of the HII regions and affect the diffuse radiation field causing the dust grains to get heated up. Thus, temperature of the cool dust component of the ISM will enable us to investigate star formation in such galaxies. In this regard, a detailed study by Davies et al. (2019) revealed a strong relation between the SFR normalized over the total dust content versus temperature of the cold dust and was reported to be steeper for the late-type galaxies relative to that for the early-type galaxies. Following this, we have also attempted to examine the dependence of the SFR per unit dust mass versus temperature of the cool dust  $T_{\text{C}}^{\text{ISM}}$  and the result is shown in the right panel of Fig. 4. This plot confirms a marginal but positive correlation between the two yielding the Pearson correlation coefficient equal to 0.24 for:

$$\log(\text{SFR}/M_{\text{dust}}) = 0.032 \log(T_{\text{C}}^{\text{ISM}}) - 8.06. \quad (4)$$

A similar positive correlation was also witnessed by Clemens et al. (2013) for a sample of star-forming galaxies from the local universe. The median values of the dust grain temperatures for the SF, Seyfert and LINER galaxies were found to be 23K, 19K and 18K, respectively.

### 3.4. Minor merger induced star formation

Though the blue ETGs from our sample exhibit strong optical emission lines and possess high SFRs, they occupy the off main-sequence positions on the CMD diagram (Fig. 3). A careful inspection of this plot reveals that the majority of the systems from our sample lie within or in the vicinity of the transition state known as the *green valley* region. This transitional state is mainly occupied by the late-type galaxies (Mendez et al. 2011) and represent the secular evolution of the blue late-type galaxies to the redder ones. However, for the case of the blue ETGs, this transitional state may be an outcome of some external trigger that pushes the red and the dead systems back to the active phase suggesting a non-secular evolution of these systems. The blue color of the ETGs is likely to be due to minor mergers, which in turn triggers the star formation in these galaxies. Evidences in support of this scenario were provided by George and Zingade (2015) through detection of the tidal interaction/merger-like signatures in 55 SF galaxies from our sample through the structural analysis. Kaviraj (2010) employing the SDSS and GALEX data on a sample of 101 spheroidal galaxies has revealed that the (NUV-*u*) and (*g* - *z*) colors of the ETGs are linked with the episodes of recent starburst which then provides a *lookback* time to the onset of the star formation due to mergers. Following Kaviraj (2010) we also investigate the probable time when the recent past starburst occurred in the sample galaxies as:

$$\log(T [\text{Gyrs}]) = 0.60 \times [(\text{NUV} - u) - (g - z) - 1.73]. \quad (5)$$

The median values of the time when merger triggered starburst in the SF, Seyfert and LINER galaxies took place are 0.13 Gyr, 0.15 Gyr, and 0.31 Gyr, respectively.

### 3.5. Possible evolutionary path of BETGs

In a recent study of 273,274 galaxies spanning over the redshift range from 0.1 to 0.4 Leslie et al. (2016) demonstrates that the galaxies follow an evolutionary pathway starting from the star-forming blue galaxy phase to the composites, Seyferts, LINERs and finally terminate in the red and dead phase. This is in line with the evolutionary path from the merger-to-the starburst-to-the AGN as predicted by (Kewley and Dopita 2003). For the case of the blue ETGs from our sample this study has evidenced the decrease in SFR and sSFR while we move over the sequence from SF - to Seyferts - to - LINERs (Fig. 3) suggesting the evolutionary sequence for them. This study has noticed a decreasing trend in the dust content and dust mass fraction over the sequence. Thus, the systematic decreasing trend of the star formation and the dust content points towards the evolutionary sequence of the blue ETGs as the SF phase to Seyferts and LINERs.

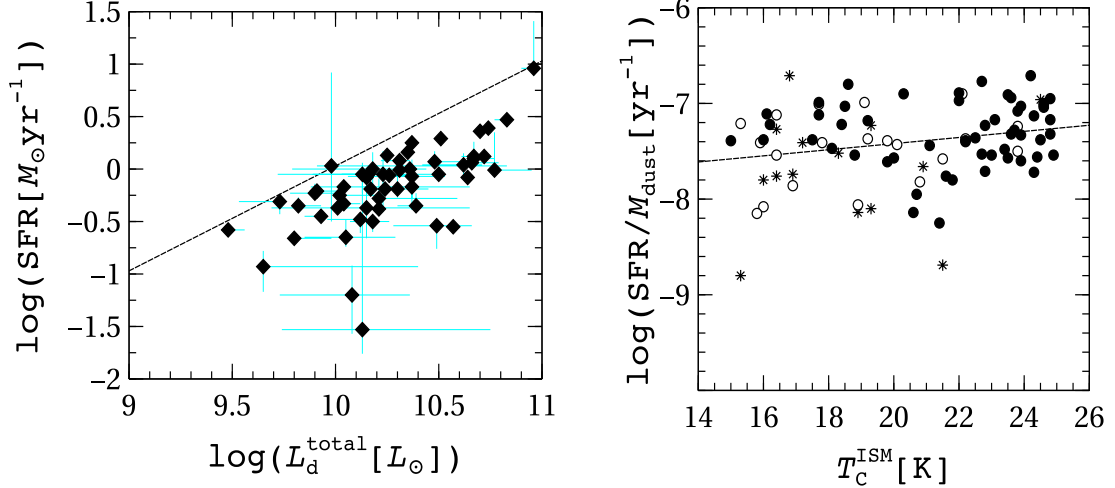


**Fig. 4:** *Left panel:* Correlation between the dust luminosity versus SFR for the SF galaxies from the present sample. The dotted line represents the correlation reported by Kennicutt (1998) for star forming galaxies. *Right panel:* The variation of the temperature of the cool dust component (i.e. the dust in ambient ISM) versus the SFR per unit dust mass. Filled circles represent the SF galaxies, open circles represent Seyferts whereas LINERs are represented by asterisks.

#### 4. CONCLUSION

This paper presents a comparative study of the physical properties of a sample of 89 blue ETGs from the local universe with redshifts in the range between  $0.02 < z < 0.05$  by fitting SEDs to their multi-wavelength photometric and spectroscopic data. The sample considered here comprises 55 star-forming galaxies, 20 Seyferts and 14 LINERs. We constructed the template-based SED fitting of the received energy over the UV to far-IR range employing the spectrophotometric multi-wavelength data from various observatories with the *MAGPHYS* and *SED3FIT* codes. This SED fitting analysis enabled us to derive various physical properties of the target galaxies like their stellar mass, dust contents, star formation rates, specific star formation rates, dust luminosities, etc. The main results from this study are summarized below:

- The detailed SED analysis of the interstellar dust extinction using corrected optical and UV flux densities enabled us to trace the evolutionary sequence of the blue BETs through the green valley.
- The median values of the dust content of the SF, Seyfert and LINERs from the present sample, respectively, are found to be equal to  $1.40 \times 10^7 M_\odot$ ,  $1.36 \times 10^7 M_\odot$ , and  $1.05 \times 10^7 M_\odot$ , respectively.
- The median values of the SFR for the SF, Seyfert and LINER galaxies, respectively, are estimated to be  $0.83 \text{ yr}^{-1}$ ,  $0.70 \text{ yr}^{-1}$ , and  $0.29 \text{ yr}^{-1}$  with the median values of the specific SFR (sSFR), respectively, equal to  $2.69 \times 10^{-11} \text{ yr}^{-1}$ ,  $1.70 \times 10^{-11} \text{ yr}^{-1}$ , and  $6 \times 10^{-12} \text{ yr}^{-1}$ , respectively.

- Despite the blue colors and strong emission lines in the optical regime of the electromagnetic spectrum, the blue ETGs in the present sample occupy position off the main sequence, commonly known as the *green valley*, on the CMD plot and hence they indicate a transitional state of their non-secular evolution.
- This study has observed a decreasing trend of the SFR, sSFR, dust mass, and dust mass fraction over the sequence from the SF - to - Seyferts - to LINERs. The UV-optical colors also enabled us to estimate the look-back time of the last starburst phase in the SF, Seyfert, and LINER galaxies, probably pointing towards the evolutionary sequence of the blue ETGs.
- A marginal positive correlation is found to be present between SFR per unit dust mass and temperature of cool ISM. Also, median values of the temperature of cool ISM are found to be lower for the AGNs as compared to SF galaxies. It indicates that the AGN component in the sample galaxies is not enough powerful to affect the host galaxy environment.

#### REFERENCES

- Abazajian, K. N., Adelman-McCarthy, J. K., Agüeros, M. A., et al. 2009, *ApJS*, **182**, 543  
 Baum, W. A. 1959, *PASP*, **71**, 106  
 Berta, S., Lutz, D., Santini, P., et al. 2013, *A&A*, **551**, A100  
 Bevington, P. R. and Robinson, D. K. 2003, Data reduction and error analysis for the physical sciences  
 Bruzual, G. and Charlot, S. 2003, *MNRAS*, **344**, 1000

- Calura, F., Pozzi, F., Cresci, G., et al. 2017, *MNRAS*, **465**, 54
- Cardelli, J. A., Clayton, G. C. and Mathis, J. S. 1989, *ApJ*, **345**, 245
- Chabrier, G. 2003, *PASP*, **115**, 763
- Charlot, S. and Fall, S. M. 2000, *ApJ*, **539**, 718
- Chen, C.-T. J. and Hickox, R. C. 2014, in IAU Symposium, Vol. 304, Multiwavelength AGN Surveys and Studies, ed. A. M. Mickaelian and D. B. Sanders, 302–306
- Cid Fernandes, R., Gu, Q., Melnick, J., et al. 2004, *MNRAS*, **355**, 273
- Cid Fernandes, R., Mateus, A., Sodré, L., Stasińska, G. and Gomes, J. M. 2005, *MNRAS*, **358**, 363
- Clauset, A., Shalizi, C. R. and Newman, M. E. J. 2009, *SIAM Review*, **51**, 661
- Clemens, M. S., Negrello, M., De Zotti, G., et al. 2013, *MNRAS*, **433**, 695
- da Cunha, E., Charlot, S. and Elbaz, D. 2008, *MNRAS*, **388**, 1595
- da Cunha, E., Eminian, C., Charlot, S. and Blaizot, J. 2010, *MNRAS*, **403**, 1894
- Davies, J. I., Nersesian, A., Baes, M., et al. 2019, *A&A*, **626**, A63
- Davis, T. A., Greene, J. E., Ma, C.-P., et al. 2019, *MNRAS*, **486**, 1404
- Deshmukh, S. P., Tate, B. T., Vagshette, N. D., Pandey, S. K. and Patil, M. K. 2013, *RAA*, **13**, 885
- Dewangan, G. C., Singh, K. P. and Bhat, P. N. 1999, *AJ*, **118**, 785
- Diamond-Stanic, A. M. and Rieke, G. H. 2012, *ApJ*, **746**, 168
- Ebneter, K. and Balick, B. 1985, *AJ*, **90**, 183
- Elbaz, D., Daddi, E., Le Borgne, D., et al. 2007, *A&A*, **468**, 33
- Faber, S. M. 1973, *ApJ*, **179**, 423
- Faber, S. M., Willmer, C. N. A., Wolf, C., et al. 2007, *ApJ*, **665**, 265
- Fabian, A. C. 2012, *ARA&A*, **50**, 455
- Finkelman, I., Brosch, N., Funes, J. G., et al. 2012, *MNRAS*, **422**, 1384
- Fritz, J., Franceschini, A. and Hatziminaoglou, E. 2006, *MNRAS*, **366**, 767
- Ge, C. and Gu, Q.-S. 2012, *RAA*, **12**, 485
- George, K. and Zingade, K. 2015, *A&A*, **583**, A103
- Gomes, J. M. and Papaderos, P. 2016, *A&A*, **594**, A49
- Goudfrooij, P., de Jong, T., Hansen, L. and Norgaard-Nielsen, H. U. 1994a, *MNRAS*, **271**, 833
- Goudfrooij, P., Hansen, L., Jorgensen, H. E. and Norgaard-Nielsen, H. U. 1994b, *A&AS*, **105**, 341
- Hjorth, J., Gall, C. and Michałowski, M. J. 2014, *ApJL*, **782**, L23
- Hopkins, A. M., Miller, C. J., Nichol, R. C., et al. 2003, *ApJ*, **599**, 971
- Huertas-Company, M., Aguerri, J. A. L., Tresse, L., et al. 2010, *A&A*, **515**, A3
- Kannappan, S. J., Guie, J. M. and Baker, A. J. 2009, *AJ*, **138**, 579
- Kaviraj, S. 2010, *MNRAS*, **408**, 170
- Kaviraj, S., Tan, K.-M., Ellis, R. S. and Silk, J. 2011, *MNRAS*, **411**, 2148
- Kennicutt, Jr., R. C. 1998, *ARA&A*, **36**, 189
- Kewley, L. J. and Dopita, M. A. 2003, in Revista Mexicana de Astronomia y Astrofisica, vol. 27, Vol. 17, Revista Mexicana de Astronomia y Astrofisica Conference Series, ed. V. Avila-Reese, C. Firmani, C. S. Frenk, and C. Allen, 83–84
- Kirkpatrick, A., Calzetti, D., Kennicutt, R., et al. 2014, *ApJ*, **789**, 130
- Knapp, G. R., Guhathakurta, P., Kim, D.-W. and Jura, M. A. 1989, *ApJS*, **70**, 329
- Kodama, T. and Arimoto, N. 1997, *A&A*, **320**, 41
- Lee, J. H., Lee, M. G. and Hwang, H. S. 2006, *ApJ*, **650**, 148
- Leslie, S. K., Kewley, L. J., Sanders, D. B. and Lee, N. 2016, *MNRAS*, **455**, L82
- Lintott, C. J., Schawinski, K., Slosar, A., et al. 2008, *MNRAS*, **389**, 1179
- Marino, A., Bianchi, L., Rampazzo, R., et al. 2011, *ApJ*, **736**, 154
- Mateus, A., Sodré, L., Cid Fernandes, R. and Stasińska, G. 2007, *MNRAS*, **374**, 1457
- McIntosh, D. H., Wagner, C., Cooper, A., et al. 2014, *MNRAS*, **442**, 533
- Mendez, A. J., Coil, A. L., Lotz, J., et al. 2011, *ApJ*, **736**, 110
- Morganti, R., de Zeeuw, P. T., Oosterloo, T. A., et al. 2006, *MNRAS*, **371**, 157
- Oke, J. B. and Gunn, J. E. 1983, *ApJ*, **266**, 713
- Oosterloo, T., Morganti, R., Crocker, A., et al. 2010, *MNRAS*, **409**, 500
- Osterbrock, D. E. 1960, *ApJ*, **132**, 325
- Patil, M. K., Pandey, S. K., Sahu, D. K. and Kembhavi, A. 2007, *A&A*, **461**, 103
- Rafferty, D. A., Brandt, W. N., Alexander, D. M., et al. 2011, *ApJ*, **742**, 3
- Rodighiero, G., Brusa, M., Daddi, E., et al. 2015, *ApJL*, **800**, L10
- Rowlands, K., Dunne, L., Maddox, S., et al. 2012, *MNRAS*, **419**, 2545
- Rutkowski, M. J., Jeong, H., Cohen, S. H., et al. 2014, *ApJ*, **796**, 101
- Salim, S. 2014, *Serb. Astron. J.*, **189**, 1
- Santini, P., Maiolino, R., Magnelli, B., et al. 2014, *A&A*, **562**, A30
- Schawinski, K., Thomas, D., Sarzi, M., et al. 2007, *MNRAS*, **382**, 1415
- Schawinski, K., Lintott, C., Thomas, D., et al. 2009, *MNRAS*, **396**, 818
- Schiminovich, D., Wyder, T. K., Martin, D. C., et al. 2007, *ApJS*, **173**, 315
- Schlegel, D. J., Finkbeiner, D. P. and Davis, M. 1998, *ApJ*, **500**, 525
- Schweizer, F. and Seitzer, P. 1992, *AJ*, **104**, 1039
- Serra, P. and Oosterloo, T. A. 2010, *MNRAS*, **401**, L29
- Skibba, R. A., Engelbracht, C. W., Dale, D., et al. 2011, *ApJ*, **738**, 89
- Skrutskie, M. F., Cutri, R. M., Stiening, R., et al. 2006,

- AJ, 131, 1163
- Smith, D. J. B., Dunne, L., da Cunha, E., et al. 2012, MNRAS, 427, 703
- Stark, D. V., Kannappan, S. J., Wei, L. H., et al. 2013, ApJ, 769, 82
- Vagshette, N. D., Pandge, M. B., Pandey, S. K. and Patil, M. K. 2012, NewA, 17, 524
- Visvanathan, N. and Sandage, A. 1977, ApJ, 216, 214
- Wei, L. H., Kannappan, S. J., Vogel, S. N. and Baker, A. J. 2010, ApJ, 708, 841
- Wong, O. I., Schawinski, K., Józsa, G. I. G., et al. 2015, MNRAS, 447, 3311
- Wright, E. L., Eisenhardt, P. R. M., Mainzer, A. K., et al. 2010, AJ, 140, 1868
- Wyder, T. K., Martin, D. C., Schiminovich, D., et al. 2007, ApJS, 173, 293
- Yi, S. K., Yoon, S.-J., Kaviraj, S., et al. 2005, ApJL, 619, L111
- York, D. G., Adelman, J., Anderson, Jr., J. E., et al. 2000, AJ, 120, 1579
- Young, L. M., Bureau, M., Davis, T. A., et al. 2011, MNRAS, 414, 940

## ОСОБИНЕ ЗВЕЗДА И ПРАШИНЕ У УЗОРКУ ПЛАВИХ ГАЛАКСИЈА РАНОГ ТИПА

S. P. Deshmukh<sup>1</sup>, N. D. Vagshette<sup>2</sup> and M. K. Patil<sup>3</sup>

<sup>1</sup>*Department of Physics, Institute of Science, civil lines, Nagpur-440001, India*

E-mail: *phy.deshmukh@iscnagpur.ac.in*

<sup>2</sup>*Department of Physics and Electronics, Maharashtra Udaygiri Mahavidyalaya, Udgir, Latur-413517, India*

E-mail: *nilkanth1384@gmail.com*

<sup>3</sup>*Swami Ramanand Teerth Marathwada University, Nanded 631 606, India*

E-mail: *patil@associates.iucaa.in*

*Оригиналан научни рад*  
УДК 524.3 + 524.57 : 524.7

Овај рад представља упоредну студију физичких особина за узорак од 89 плавих галаксија раног типа из локалног универзума, користећи фитовање укупне спектралне енергетске дистрибуције (SED) спектроскопским и фотометријским посматрањима на више таласних дужина. Детаљно фитовање SED на основу базе репрезентативних узорака користећи кодове MAGPHYS и SED3FIT на спектрофотометријским посматрањима која покривају од UV до далеког IR дела спектра, и која су коригована за екстинкцију међузвезданом прашином, омогућило нам је мапирање еволуционе фазе плавих галаксија раног типа на дијаграму боја-магнитуда. Ова студија показује опадајући тренд стопе формирања звезда, специфичне стопе формирања звезда, масе прашине и удела прашине у укупној маси, посматрано од галаксија које формирају звезде, преко Сејфертових, па све до LINER галаксија. UV-оптичке боје омогућиле су нам да про-

ценимо време протекло од последње фазе формирања звезда у поменутом три типа галаксија - активним у формирању звезда, Сејфертовим и LINER галаксијама, вероватно указујући на смер еволуције плавих галаксија раног типа. Упркос плавој боји и јаким емисионим линијама у оптичком делу EM спектра, плаве галаксије раног типа у посматраном узорку заузимају фазу ван Главног низа, уобичајено названу Зелена долина на дијаграму боја-магнитуда, и зато указују да је ова фаза пролазна у несекуларној еволуцији. Занемарљива позитивна корелација је запажена између стопе формирања по јединици масе прашине и температуре хладне међузвездане материје. Опадајући тренд температуре хладне прашине  $T_c$ , почевши од галаксија које формирају звезде, преко Сејфертових, до LINER, указује да њихова активна галактичка језгра нису довољно снажна да утичу на хладну компоненту међузвездане материје.